

**Transmission of intense femtosecond laser pulses into dielectrics**J. R. Peñano,<sup>1</sup> P. Sprangle,<sup>1</sup> B. Hafizi,<sup>2</sup> W. Manheimer,<sup>2</sup> and A. Zigler<sup>2</sup><sup>1</sup>*Plasma Physics Division, Naval Research Laboratory, Washington, DC 20375, USA*<sup>2</sup>*Icarus Research, Inc., P.O. Box 30780, Bethesda, Maryland 20824-0780, USA*

(Received 24 February 2005; published 23 September 2005)

The interaction of intense, femtosecond laser pulses with a dielectric medium is examined using a numerical simulation. The simulation uses the one-dimensional electromagnetic wave equation to model laser pulse propagation. In addition, it includes multiphoton ionization, electron attachment, Ohmic heating of free electrons, and temperature-dependent collisional ionization. Laser pulses considered in this study are characterized by peak intensities  $\sim 10^{12}$ – $10^{14}$  W/cm<sup>2</sup> and pulse durations  $\sim 10$ – $100$  fsec. These laser pulses interacting with fused silica are shown to produce above-critical plasma densities and electron energy densities sufficient to attain experimentally measured damage thresholds. Significant transmission of laser energy is observed even in cases where the peak plasma density is above the critical density for reflection. A damage fluence based on absorbed laser energy is calculated for various pulse durations. The calculated damage fluence threshold is found to be consistent with recent experimental results.

DOI: [10.1103/PhysRevE.72.036412](https://doi.org/10.1103/PhysRevE.72.036412)

PACS number(s): 52.38.–r, 42.65.Re, 52.50.Jm, 42.25.Bs

**I. INTRODUCTION**

The interaction of high-intensity femtosecond laser pulses with dielectric materials involves a number of physical mechanisms that occur on time scales comparable with both the laser frequency and pulse duration and spatial scales that can be shorter than the laser wavelength. For example, the electron collision time can be comparable with the optical laser period and the width of the plasma layer generated at the dielectric surface can be much less than an optical wavelength [1]. In addition, the collisional ionization time of the dielectric surface is comparable with the pulse duration. In these situations an accurate description of laser pulse propagation is necessary to describe the interaction and subsequent transmission of laser energy into the dielectric.

A high-intensity ( $>10^{13}$  W/cm<sup>2</sup>), ultrashort ( $\sim 100$  fsec) laser pulse impinging on a dielectric surface initially generates free electrons (plasma) through multiphoton or tunneling ionization. For the femtosecond time scales involved, these electrons gain energy from the laser field through collisional heating. As the electron temperature increases the collisional ionization rate also increases. The plasma density generated on the dielectric surface can be greater than the critical density for reflecting the laser pulse. The photoionization and collisional ionization process for femtosecond laser pulses has been studied extensively both theoretically [1–5] and experimentally [1,6–10]. Theoretical descriptions of the collisional ionization process range in complexity and include fully kinetic models [4], models which make the flux-doubling assumption [1,10], and multiple-rate-equation descriptions [5].

In these previous studies, laser propagation is treated in an approximate fashion; i.e., the electric field in the dielectric is taken to be evanescent and the ionization equations are solved purely in the time domain at a given spatial position for a given temporal laser profile. Stuart *et al.* [1] considered a limited laser propagation model involving the steady-state form of the transmission coefficient to calculate the transmit-

ted laser pulse shape and energy deposition depth. That study, using 1053-nm- and 526-nm-wavelength, subpicosecond pulses, predicted above-critical plasma densities and plasma layer widths smaller than the laser wavelength. For a laser pulse with 1053 nm wavelength,  $\sim 200$  fsec duration, and 3.5 J/cm<sup>2</sup> fluence—i.e., above the damage threshold—Stuart's propagation model predicted significant absorption of laser energy ( $\sim 60\%$ ) within 1  $\mu\text{m}$  of the surface.

Here, we utilize a fully time-dependent theoretical model to simulate the interaction of a high-intensity, femtosecond laser pulse with a dielectric. We model the propagation of the laser in one dimension (1D) using the electromagnetic wave equation coupled to an equation for the induced plasma current. The plasma is generated by multiphoton and collisional (avalanche) ionization. The collisional ionization process is described by a reduced kinetic model which allows us to write a temperature-dependent ionization rate in closed form. The plasma electrons are heated by the laser field via collisions with ions and neutrals. For femtosecond laser pulses, the absorbed electromagnetic energy of the laser is mainly converted to kinetic energy of free electrons. The hot plasma layer formed on the surface of the dielectric is typically much smaller in width than an optical wavelength. The heated electrons transfer their energy to the lattice on a time scale much longer than the laser pulse duration [1].

The model equations are solved numerically to determine laser pulse transmission, laser energy absorption, damage thresholds, and plasma density, and temperature within the dielectric. Our results show much greater transmission compared with a purely steady-state calculation. The enhanced transmission is due to the fact that the critical density for reflection is generated only after a significant part of the pulse has crossed the surface boundary. To a lesser degree, the high collisionality of the plasma layer also enhances transmission. The transmission of laser energy through the plasma layer has applications to the operation and design of plasma-based switches and mirrors [11] and possibly electronic countermeasures.

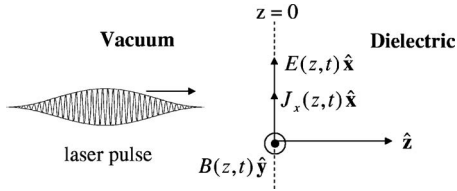


FIG. 1. Schematic illustration of the numerical model geometry.

In this study we consider laser intensities of  $10^{13}$ – $10^{14}$  W/cm<sup>2</sup> and pulse durations from tens to hundreds of femtoseconds—i.e., pulses that can be propagated many tens of meters in air [12]. We limit our study to parameter regimes for which thermal and particle diffusion, nonlinear self-focusing, and group velocity dispersion can be neglected. We note that others have used full particle-in-cell simulations to model laser propagation in dielectrics, although the parameter regimes investigated are different from what is considered here [13]. Experimentally, the transmission of focused, intense femtosecond laser pulses through fused silica was observed by von der Linde and Schueler [14].

Section II of the paper discusses the theoretical model. Section III presents the results and compares with experimental data from single-pulse interactions with fused silica. Conclusions are presented in Sec. IV.

## II. THEORETICAL MODEL

We consider the situation in which a laser pulse propagating along the  $z$  axis is incident on a dielectric which is located at  $z > 0$ , as shown in Fig. 1. The laser intensity is high enough that it can singly ionize the dielectric and heat the resulting plasma. The laser electric field  $\mathbf{E} = E(z,t)\hat{\mathbf{x}}$  and magnetic field  $\mathbf{B} = B(z,t)\hat{\mathbf{y}}$  are determined by the Maxwell equations

$$n_0^2(z,t) \frac{\partial E}{\partial t} = -c \frac{\partial B}{\partial z} - 4\pi [J_x(z,t) + J_{mpi}(z,t)], \quad (1a)$$

$$\frac{\partial B}{\partial t} = -c \frac{\partial E}{\partial z}, \quad (1b)$$

where the source current  $J_x$  denotes the linear plasma response and  $J_{mpi}$  is an effective current which accounts for laser energy depletion due to multiphoton ionization [15]. The refractive index is given by a low-frequency Lorentz model—i.e.,  $n_0^2(z,t) = 1 + \omega_n^2(z,t)/\Omega_0^2$ , where the quantity  $\Omega_0$  is a constant that determines the magnitude of the refractive index in the absence of ionization,

$$\omega_n(z,t) = \sqrt{4\pi q^2 n_n(z,t)/m},$$

and  $n_n(z,t)$  is the density of neutrals. In writing the refractive index this way, dispersion is neglected.

The linear transverse plasma current is given by

$$\frac{\partial J_x}{\partial t} = -\nu_e J_x + \frac{\omega_p^2(z,t)}{4\pi} E, \quad (2)$$

where  $\omega_p(z,t) = \sqrt{4\pi q^2 n_e(z,t)/m}$  is the electron plasma frequency and  $n_e$  is the electron density. Equation (2) is exact for the case of a cold plasma in which free electrons are created with zero mean momentum [15]. Viscosity effects have also been neglected. The electron collision frequency  $\nu_e = \nu_{ei} + \nu_{en}$  is the sum of the electron-neutral and electron-ion collision frequencies which are given by

$$\nu_{en} [\text{sec}^{-1}] = 2 \times 10^{-7} n_n [\text{cm}^{-3}] T_e^{1/2} [\text{eV}], \quad (3a)$$

$$\nu_{ei} [\text{sec}^{-1}] = 2.91 \times 10^{-6} Z n_e [\text{cm}^{-3}] \Lambda(n_e, T_e) T_e^{-3/2} [\text{eV}], \quad (3b)$$

respectively, where  $\Lambda(n_e, T_e)$  is the Coulomb logarithm and  $T_e$  is the electron temperature [16]. For this study, we limit  $\Lambda$  to values greater than 2.

The plasma generation is described by

$$\frac{\partial n_e}{\partial t} = \nu_m(E) n_n + \nu_{col}(T_e, n_n) n_e - n_e / \tau_{trap}, \quad (4)$$

where  $\nu_m$  and  $\nu_{col}$  are the multiphoton and collisional ionization rates, respectively. For this study, we use the six-photon ionization rate for the interaction of  $0.8 \mu\text{m}$  radiation with fused silica (ionization energy  $W_{ion} = 9$  eV),

$$\nu_m [\text{sec}^{-1}] = \frac{\sigma_6 I^6}{n_{n0}}, \quad (5)$$

where  $\sigma_6 = 2 \times 10^{13} \text{ cm}^{-3} \text{ psec}^{-1} (\text{cm}^2/\text{TW})^6$  [17] is the Keldysh six-photon ionization coefficient,  $n_{n0}$  is the neutral density in the absence of ionization, and  $I$  is the slowly varying, time-averaged laser intensity. It is assumed that only single ionization of neutrals occurs. This assumption will not significantly affect the transmission of the laser pulse since all transmission occurs before the saturation of ionization; i.e., the critical density for reflection is approximately 3 times lower than the maximum ionization density.

The exponential decay of electron density, given by the third term on the right side of Eq. (4), has been observed experimentally with a characteristic decay time  $\tau_{trap} = 150$  fsec [18]. Physically, the overall decay in electron density is due to a number of processes—e.g., recombination, attachment, diffusion.

The current density  $J_{mpi}$  can be derived by equating the time rate of change of laser energy density due to multiphoton ionization with the product  $J_{mpi} E$ . The result is [15]

$$J_{mpi} = W_{ion} \nu_m(E) n_n / E, \quad (6)$$

where  $W_{ion}$  is the ionization energy.

The collisional ionization rate can be written as  $\nu_{col} = \int_0^\infty \nu_0(W) f_e(W) dW$ , where  $f_e$  is the electron energy distribution function and  $\nu_0(W) = \alpha_0 (W/W_{ion} - 1)^2$  for  $W \geq W_{ion}$  and zero for  $W < W_{ion}$  [2]. The rate constant  $\alpha_0$  is particular to the material under consideration and can be empirically determined. For fused silica,  $\alpha_0 = 1.5 \text{ fsec}^{-1}$  [1,19]. We assume a Maxwellian distribution for the electron velocity—i.e.,

$F(\nu) = (\pi^{1/2} \nu_{th})^{-3} \exp(-\nu^2/\nu_{th}^2)$ . The corresponding energy distribution function is

$$f_e(W) = 2 \left( \frac{W}{\pi W_{th}^3} \right)^{1/2} \exp(-W/W_{th}),$$

where  $W_{th} = m\nu_{th}^2/2 = 3k_B T_e/2$  and  $f_e(W)$  is normalized such that  $\int_0^\infty f_e(W) dW = 1$ . Using this distribution function, the collisional ionization rate is given by

$$\nu_{col}(\beta) = \frac{2\alpha_0 n_n}{\sqrt{\pi} n_{n0}} \left[ \left( \frac{15}{4} \beta^{3/2} - \frac{1}{2} \beta^{1/2} \right) \exp(-1/\beta) + \frac{\sqrt{\pi}}{2} \left( \frac{15}{4} \beta^2 - 3\beta + 1 \right) \operatorname{erfc}(1/\sqrt{\beta}) \right], \quad (7)$$

where  $\beta = W_{th}/W_{ion}$  and  $\operatorname{erfc}(x) = 1 - (2/\sqrt{\pi}) \int_0^x \exp(-t^2) dt$  denotes the complementary error function.

For the parameter regime considered here, thermal conduction can be neglected and the electron thermal energy satisfies the equation

$$\frac{\partial(n_e W_{th})}{\partial t} = J_x E - \Gamma W_{ion} \nu_{col} n_e. \quad (8)$$

The first term on the right side of Eq. (8) represents Ohmic heating of the electrons while the second term represents the energy lost by free electrons due to collisional ionization. The constant  $\Gamma$  takes into account the fact that due to other electronic excitations, it usually requires energies greater than  $W_{ion}$  to ionize by collisions. For example, in gas discharges,  $2 < \Gamma < 5$  for electron energies comparable with the ionization energy [20]. Here, we take  $\Gamma = 2$  as a canonical value. Equation (8) implicitly assumes that electrons generated by multiphoton ionization are created with zero kinetic energy; i.e., above threshold ionization is neglected. It is also assumed that in the electron decay process, an electron that is captured transfers its kinetic energy to another electron. This is apparent from the lack of a cooling term in Eq. (8) that is proportional to the electron decay rate  $1/\tau_{trap}$ .

### III. RESULTS

Equations (1), (2), (4), and (8) are solved numerically using a finite-difference, staggered leapfrog approach. In what follows we consider laser pulses with wavelength  $\lambda = 0.8 \mu\text{m}$ , durations ranging from 30 to 400 fsec, and fluences  $< 6 \text{ J/cm}^2$ . The temporal profile of the laser electric field with carrier frequency  $\omega_0$  at a fixed  $z$  position in vacuum ( $z < 0$ ) is given by

$$E(z < 0, t) = E_0 \sin[\pi t/\tau_L] \cos\{\omega_0[t - (\tau_L/2)]\} \quad (9)$$

for  $0 < t < \tau_L$  and zero otherwise. The full width at half maximum of intensity is given by  $\tau_{FWHM} = \tau_L/2$ .

The laser pulse is made to interact with a dielectric located in the region  $z > 0$ . The dielectric is taken to be fused silica—i.e., refractive index  $n_0 = 1.5$ , ionization energy  $W_{ion} = 9 \text{ eV}$ , and neutral density  $n_{n0} = 2 \times 10^{22} \text{ cm}^{-3}$ . The ionization rate constant is  $\alpha_0 = 1.5 \text{ fsec}^{-1}$  [1,19]. For the assumed wavelength and ionization energy, multiphoton ionization is

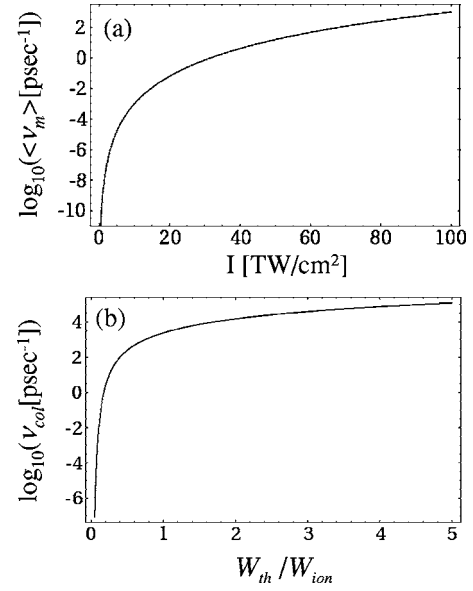


FIG. 2. (a) Multiphoton ionization rate versus laser intensity according to Eq. (5). (b) Collisional ionization rate versus  $W_{th}/W_{ion}$  according to Eq. (7). The neutral density for both figures is taken to be  $n_n = 2 \times 10^{22} \text{ cm}^{-3}$  and  $\alpha_0 = 1.5 \text{ fsec}^{-1}$ .

a six-photon process where the ionization rate is described by Eq. (5). Figure 2 plots the multiphoton ionization rate as a function of laser intensity [Fig. 2(a)] and the collisional ionization rate as a function of  $\beta \equiv W_{th}/W_{ion}$  [Fig. 2(b)] for the assumed dielectric parameters.

#### A. Steady-state solution

Laser pulses that are sufficiently intense will ionize the dielectric surface, producing a thin plasma layer that can reflect and absorb laser energy. Before we solve the fully time-dependent problem including ionization, we first consider the steady-state interaction of a laser with a preexisting thin, highly collisional plasma layer on the surface of a dielectric and calculate the transmission of the laser into the dielectric. We take the region  $z < 0$  to be a vacuum, the region from  $0 < z < L$  to contain a pre-ionized dielectric with a given electron temperature, and the region  $z > L$  to contain a dielectric of refractive index  $n_0$ . Ionization and heating by the laser pulse are neglected in this simplified steady-state model. It is assumed that the regions  $z < 0$  and  $0 < z < L$  contain right- and left-going waves, while only a transmitted (right-going) wave exists in the region  $z > L$ . The electron collision frequency is calculated according to Eqs. (3). If the plasma density and temperature within the region  $0 < z < L$  are uniform, the transmitted intensity for  $z > L$  can be calculated analytically. The curve in Fig. 3 shows the transmitted intensity (normalized to the incident intensity) versus the ratio  $\omega_p/\omega_0$ . In generating this curve, we use parameters characteristic of the fully time-dependent simulations presented later—i.e., electron temperature of 10 eV,  $n_0 = 1.5$ ,  $\lambda = 0.8 \mu\text{m}$ , and  $L = \lambda/10$ . It is seen that for maximum ionization—i.e.,  $\omega_p = 3.4\omega_0$ —the steady-state calculation predicts a fractional transmission of  $\sim 3 \times 10^{-2}$ .

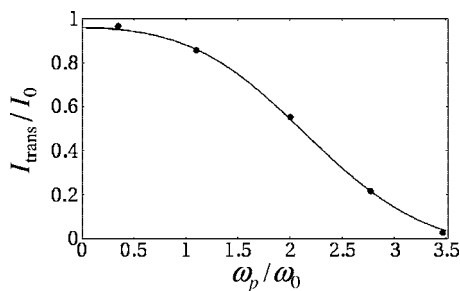


FIG. 3. Steady-state transmitted intensity normalized to the incident intensity versus normalized plasma frequency for  $\lambda = 0.8 \mu\text{m}$  radiation impinging on a dielectric ( $n_0 = 1.5$ ) with a preformed surface plasma layer of width  $L = \lambda/10$  and electron temperature of 10 eV. Ionization and heating by the laser pulse are neglected. Solid curve denotes analytic result, dots denote simulation results.

In the following section, we show that significantly higher transmission is observed when the fully time-dependent equations are solved. To benchmark the time-dependent numerical code, we simulate the steady-state interaction described above. The results of the simulation are denoted by the dots in Fig. 3. Excellent agreement is obtained with the analytic result.

### B. Time-dependent simulations

We now consider the fully time-dependent numerical solution of Eqs. (1), (2), (4), and (8). Figure 4 shows a simulation in which a laser pulse with  $\tau_L = 100$  fsec and fluence  $3.2 \text{ J/cm}^2$  ( $I_0 = 1.1 \times 10^{14} \text{ W/cm}^2$ ) impinges on fused silica. Figure 4(a) shows the spatial profile of the laser electric field before the interaction with the dielectric located in the region  $z > 0$ . After interaction with the dielectric surface, reflected

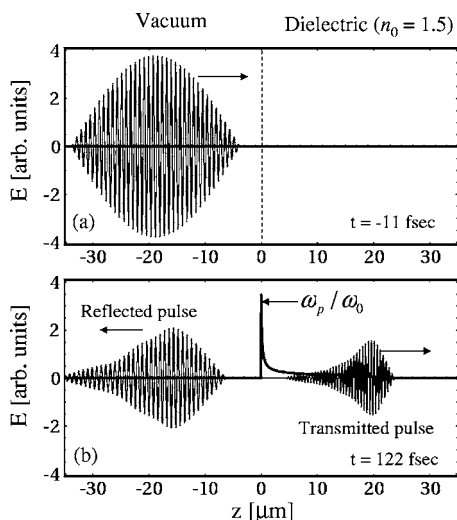


FIG. 4. (a) Initial laser field  $E$  vs  $z$  before the interaction.  $t = 0$  defines the time at which the leading edge of the pulse reaches the dielectric surface located at  $z = 0$ . (b) Electric field of the transmitted and reflected pulses  $t = 122$  fsec after the interaction. Darker curve denotes  $\omega_p/\omega_0$  vs  $z$ . Pulse duration is  $\tau_L = 100$  fsec, with fluence  $3.2 \text{ J/cm}^2$ .

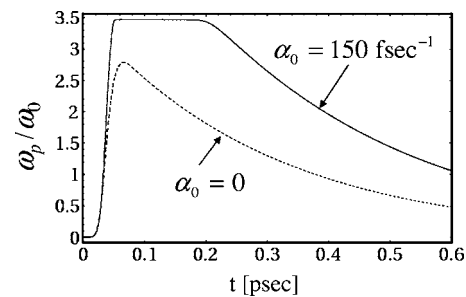


FIG. 5. Peak value of  $\omega_p/\omega_0$  vs time for cases of multiphoton ionization only ( $\alpha_0 = 0$ ), and both multiphoton and collisional ionization ( $\alpha_0 = 150 \text{ fsec}^{-1}$ ). Pulse duration is  $\tau_L = 100$  fsec, with fluence  $3.2 \text{ J/cm}^2$ .

and transmitted pulses are observed, as shown in Fig. 4(b). A plasma layer is generated with a maximum plasma frequency  $\omega_p = 3.4\omega_0$ , which corresponds to full ionization of the dielectric surface. The half-maximum width of the plasma layer is  $\sim 0.2 \mu\text{m}$ . A portion of the plasma layer near the surface is strongly heated by the laser pulse. For this particular simulation the electron temperature reaches a peak value of  $\sim 10$  eV. The half-maximum width of the heated electron layer is  $\sim 0.05 \mu\text{m}$ .

Even when the plasma density is above critical—i.e.,  $\omega_p > \omega_0$ —approximately 30% of the incident laser energy is transmitted through the surface as a propagating pulse. The transmitted pulse is steepened at the leading edge and elongated at the back. It continues to ionize the dielectric as it propagates. However, its intensity is sufficiently low that the plasma density remains well below the critical value. The spatial profile of the reflected pulse shows a gradual rise in amplitude at the front followed by a sharper rise towards the middle of the pulse, indicating a sudden increase in the reflectivity of the surface.

Figure 5 plots the normalized plasma density at the surface versus time for the simulation shown in Fig. 4. The laser pulse is located in the region  $0 < t < 100$  fsec. The plasma density reaches the critical value  $\sim 40$  fsec into the interaction. Hence, the sharp rise in the reflected pulse amplitude seen in Fig. 4 is coincident with the plasma density reaching the critical value. For comparison, Fig. 5 also plots the plasma density versus time for purely multiphoton ionization ( $\alpha_0 = 0$ ). Comparison of the two curves shows that collisional ionization increases the peak plasma density by 30%. Hence, while photoionization is the dominant ionization mechanism, collisional ionization also plays an important role.

Figure 6 shows the peak plasma density [Fig. 6(a)], fractional transmitted fluence [Fig. 6(b)], and fractional reflected fluence [Fig. 6(c)] from several simulations utilizing different pulse durations and intensities. Transmitted fluence is measured at position  $z = 1 \mu\text{m}$ . At smaller incident fluences, for which ionization is negligible—i.e.,  $\omega_p \ll \omega_0$ —the pulse is reflected and transmitted according to Snell's law. At higher fluences, when ionization becomes important, more of the laser energy is reflected and the transmission decreases. However, greater than 70% transmission of fluence is observed even when the plasma density reaches the critical density. Greater than 40% transmission can still occur when the dielectric is fully ionized ( $\omega_p = 3.4\omega_0$ ).



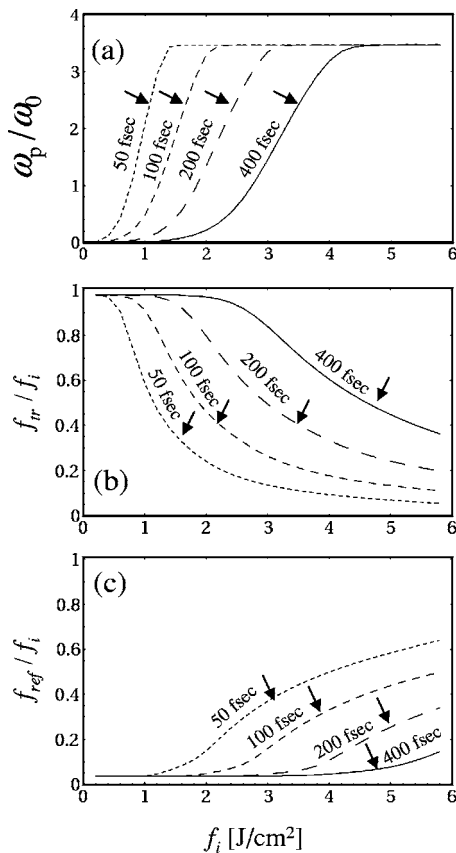


FIG. 6. (a) Normalized plasma frequency, (b) transmitted fluence  $f_{tr}/f_i$ , and (c) reflected fluence  $f_{ref}/f_i$  versus incident fluence  $f_i$  for pulse durations  $\tau_L=50, 100, 200,$  and  $400$  fsec. Transmitted fluence was recorded at position  $z=1 \mu\text{m}$ .

Strong absorption of laser energy occurs near the surface. The amount of laser energy absorbed depends on the duration and intensity of the incident laser pulse. In Fig. 7, we plot the fluence absorbed within  $1 \mu\text{m}$  of the surface versus incident fluence for various pulse lengths. The absorbed fluence is calculated as the incident fluence minus the sum of the reflected and transmitted fluences, where the transmitted fluence is measured at  $z=1 \mu\text{m}$ . The parameters are the same as in Fig. 6. It is seen that for smaller incident fluences,  $\omega_p \ll \omega_0$ , and there is no significant absorption of laser energy. As the laser intensity is increased for a fixed pulse duration, ionization occurs and the dielectric surface becomes highly

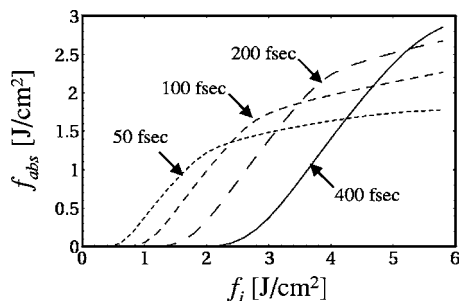


FIG. 7. Fluence absorbed within the dielectric from  $z=0$  to  $z=1 \mu\text{m}$  for the same parameters as Fig. 6.

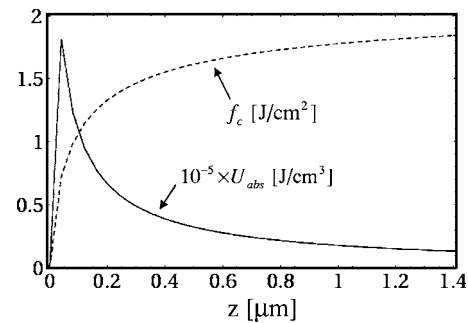


FIG. 8. Cumulative absorbed laser fluence  $f_c$  and absorbed energy density  $U_{abs}$  versus  $z$  at time  $t=122$  fsec for the same parameters as Fig. 4.

absorptive when  $\omega_p > \omega_0$ . Figure 6 shows that for incident fluence  $< 2 \text{ J/cm}^2$ , short pulses deposit energy into the dielectric more efficiently than long pulses.

Since the transition from transparency to opacity occurs very rapidly, we have also tried slightly different pulse shapes to see if the reflection and transmission would be significantly affected. We have run simulations with smoother sine-squared field profiles and found only small changes to the transmission and reflection coefficients. For example, for the case of a 100-fsec pulse the reflection coefficient increases by  $\sim 10\%$  with the smoother pulse shape.

### C. Damage threshold

Experimentally, damage has been characterized as an observable modification of the surface when viewed through a Nomarski microscope [1,8]. Experimental results also suggest that a minimum energy density must be deposited within the material in order to cause observable damage. The energy density barrier for fused silica is  $U_b=54 \text{ kJ/cm}^3$  [10].

Using our simulation, we can define a damage threshold based directly on energy absorption. Let  $f_c(z_0)$  denote the total (cumulative) laser fluence ( $\text{J/cm}^2$ ) absorbed within a layer  $0 < z < z_0$ . The energy density absorbed by the dielectric is then given by  $U_{abs}=f_c(z_0)/z_0$ . We define the damage fluence  $f_d$  as the minimum incident laser fluence required to achieve  $U_{abs}=U_b$ . Figure 8 plots  $f_c(z)$  and  $U_{abs}(z)$  for the same parameters as Fig. 4. The dependence of  $f_{abs}$  on  $z$  indicates that most of the laser absorption takes place within  $\sim 0.5 \mu\text{m}$  of the surface. The maximum absorbed energy density is  $\sim 180 \text{ kJ/cm}^3$ , which is well above what is required for damage.

Other analyses have defined the damage fluence as the minimum incident fluence required to create a plasma with a density such that  $\omega_p=\omega_0$ , arguing that the plasma becomes highly absorptive when the critical density is attained. However, because the plasma density can reach the critical density after a significant portion of the laser pulse has already passed through the plasma layer, the condition  $\omega_p=\omega_0$  may be insufficient for femtosecond laser pulses. For example, a 100-fsec laser pulse with an incident fluence of  $\sim 1.3 \text{ J/cm}^2$  can create a plasma with the critical density [see Fig. 6(a)]. However, the maximum absorbed energy density for this interaction is  $\sim 2.5 \text{ kJ/cm}^3$ , which is much less than  $U_b$ .

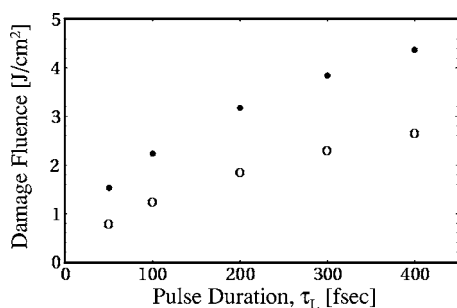


FIG. 9. Damage fluence  $f_d$  versus pulse duration  $\tau_L$  for fused silica. The damage fluence denoted by the solid dots is defined as the minimum incident fluence required to absorb  $54 \text{ kJ/cm}^3$  of laser energy within the dielectric. The damage fluence denoted by open circles is defined as the incident fluence required to create a plasma with  $\omega_p = \omega_0$ .

Figure 9 plots the damage fluence  $f_d$  calculated using two different definitions versus pulse duration. The solid dots denote the damage fluence calculated according to our definition. The open circles denote the fluence required to create a plasma with  $\omega_p = \omega_0$ —i.e., the damage fluence as defined in Refs. [1,6–8]. The damage fluence is seen to increase with pulse duration from  $\sim 1.4 \text{ J/cm}^2$  to  $4.4 \text{ J/cm}^2$  over the range  $50 \text{ fsec} < \tau_L < 400 \text{ fsec}$ . The damage fluence denoted by the open circles is lower by approximately 40% over this range of pulse durations. For example, for a pulse duration of  $\tau_L = 100 \text{ fsec}$ , it requires  $\sim 2.2 \text{ J/cm}^2$  of incident laser fluence to cause  $54 \text{ kJ/cm}^3$  of laser energy to be absorbed within the dielectric.

#### IV. CONCLUSIONS

The interaction of intense femtosecond pulses with a dielectric surface has been numerically modeled in 1D using the electromagnetic wave equation, rate equations for the electron density, and an equation describing electron energy density. The rate equations contain multiphoton ionization,

collisional ionization, and electron trapping. The equation for the electron energy density describes Ohmic heating and cooling by collisional ionization. Because the simulation solves the time-dependent electromagnetic wave equation, the transmission, reflection, and absorption of the laser pulse by a thin, highly collisional plasma layer is modeled for the first time in this parameter regime in a fully self-consistent manner. Significant differences are observed between the fully time-dependent simulation and the approximate steady-state model. It is seen that, due to the time dependence of the ionization process, a significant transmission of laser energy is possible even when the plasma density is above the critical value. This is because the density can exceed the critical value towards the trailing end of the laser pulse. For example, consider the transmission of a pulse with  $\tau_L = 100 \text{ fsec}$  and fluence of  $3.2 \text{ J/cm}^2$ . The interaction of this pulse with the dielectric fully ionizes the surface and heats the plasma to  $\sim 10 \text{ eV}$ . From Fig. 6(b) the fractional transmission of this pulse is  $\sim 25\%$  according to the time-dependent solution, while the corresponding steady-state calculation (Fig. 3) predicts a fractional transmission of only 3%.

The simulations also show that, for parameters characteristic of recent experiments using fused silica, the absorbed energy density is sufficient to cause observable damage. Our damage fluences are in good agreement with the experiments of Refs. [7,8]. We note, however, that the damage fluence in those experiments was defined as the incident fluence required to cause observable discoloration of the surface when observed through a Nomarski microscope. For our simulations, the damage threshold is defined as the incident fluence required to deposit an energy density of  $54 \text{ kJ/cm}^3$  within the material [10]. This energy density is sufficient to break a significant number of the molecular bonds near the surface.

#### ACKNOWLEDGMENT

This work was sponsored by the Office of Naval Research.

- 
- [1] B. C. Stuart, M. D. Feit, S. Herman, A. M. Rubenchik, B. W. Shore, and M. D. Perry, *Phys. Rev. B* **53**, 1749 (1996).
  - [2] L. V. Keldysh, *Sov. Phys. JETP* **37**, 509 (1960).
  - [3] K. K. Thornber, *J. Appl. Phys.* **52**, 279 (1981).
  - [4] A. Kaiser, B. Rethfeld, M. Vicanek, and G. Simon, *Phys. Rev. B* **61**, 11437 (2000).
  - [5] B. Rethfeld, *Phys. Rev. Lett.* **92**, 187401 (2004).
  - [6] D. Du, X. Liu, G. Korn, J. Squier, and G. Mourou, *Appl. Phys. Lett.* **64**, 3071 (1994).
  - [7] M. Lenzner, J. Krüger, S. Sartania, Z. Cheng, Ch. Spielmann, G. Mourou, W. Kautek, and F. Krausz, *Phys. Rev. Lett.* **80**, 4076 (1998).
  - [8] A.-C. Tien, S. Backus, H. Kapteyn, M. Murnane, and G. Mourou, *Phys. Rev. Lett.* **82**, 3883 (1999).
  - [9] E. G. Gamaly, A. V. Rode, V. T. Tikhonchuk, and B. Luther-Davies, *Appl. Surf. Sci.* **197–198**, 699 (2002).
  - [10] T. Q. Jia, Z. Z. Xu, X. X. Li, R. X. Li, B. Shuai, and F. L. Zhao, *Appl. Phys. Lett.* **82**, 4382 (2003); T. Q. Jia, Z. Z. Xu, R. X. Li, D. H. Feng, X. X. Li, C. F. Cheng, H. Y. Sun, N. S. Xu, and H. Z. Wang, *J. Appl. Phys.* **95**, 5166 (2004).
  - [11] D. M. Gold, *Opt. Lett.* **19**, 2006 (1994); B. Dromey, S. Kar, M. Zepf, and P. Foster, *Rev. Sci. Instrum.* **75**, 645 (2004).
  - [12] A. Braun, G. Korn, X. Liu, D. Du, J. Squier, and G. Mourou, *Opt. Lett.* **20**, 73 (1995); B. La Fontaine, F. Vidal, Z. Jiang, C. Y. Chien, D. Comtois, A. Desparois, T. W. Johnston, J.-C. Kieffer, H. Pepin, and H. P. Mercure, *Phys. Plasmas* **6**, 1615 (1999); M. Rodriguez, R. Bourayou, G. Méjean, J. Kasparian, J. Yu, E. Salmon, A. Scholz, B. Stecklum, J. Eisloffel, U. Laux, A. P. Hatzes, R. Sauerbrey, L. Woste, and J.-P. Wolf, *Phys. Rev. E* **69**, 036607 (2004).
  - [13] A. J. Kemp, R. E. W. Pfund, and J. Meyer-ter-Vehn, *Phys. Plasmas* **11**, 5648 (2004); A. Zhidkov and A. Sasaki, *ibid.* **7**,

- 1341 (2000).
- [14] D. von der Linde and H. Schüler, *J. Opt. Soc. Am. B* **13**, 216 (1996).
- [15] S. C. Rae and K. Burnett, *Phys. Rev. A* **46**, 1084 (1992); P. Mulser, F. Cornolti, and D. Bauer, *Phys. Plasmas* **5**, 4466 (1998).
- [16] *NRL Plasma Formulary*, edited by J. D. Huba, Naval Research Laboratory Publication NRL/PU/6790-98-358 (U.S. GPO, Washington, D.C., 1998).
- [17] L. V. Keldysh, *Sov. Phys. JETP* **20**, 1307 (1965); L. Sudrie, A. Couairon, M. Franco, B. Lamouroux, S. Tzortzakis, and A. Mysyrowicz, *Phys. Rev. Lett.* **89**, 186601 (2002).
- [18] P. Audebert, Ph. Daguzan, A. Dos Santos, J. C. Gauthier, J. P. Geindre, S. Guizard, G. Hamoniaux, K. Krastev, P. Martin, G. Petite, and A. Antonetti, *Phys. Rev. Lett.* **73**, 1990 (1994).
- [19] D. Arnold, E. Cartier, and D. J. Di Maria, *Phys. Rev. B* **45**, R1477 (1992).
- [20] M. A. Lieberman, *Principles of Plasma Discharges and Materials Processing* (Wiley, New York, 1994).